Available online at www.sciencedirect.com
ScienceDirect
Journal of Organometallic Chemistry 692 (2007) 1110–1117
Journal of Organometallic Chemistry
www.elsevier.com/locate/jorganchem

Chiral memory effects in catalytic hydrogenations with dynamically chiral ligands

J.W. Faller *, Philip P. Fontaine

Yale University, P.O. Box 208107, New Haven, CT 06520-8107, United States

Received 24 August 2006; received in revised form 6 November 2006; accepted 6 November 2006
Available online 16 November 2006

Abstract

The low barrier for interconversion of chiral conformations of the dynamically chiral 2,2′-biphenyl ligand $NMe_2C_6H_4C_6H_4PCy_2$ is raised upon coordination. The individual enantiomers of the planar chiral arene-tethered complex $Ru(\eta^6{:}\eta^1\text{-}NMe_2C_6H_4C_6H_4PCy_2)Cl_2$ (**1**), however, do not undergo racemization readily. A second source of chirality, such as a chiral diamine, can be included by conversion of **1** into a dicationic analogue $[Ru(\eta^6{:}\eta^1\text{-}NMe_2C_6H_4C_6H_4PCy_2)((1S,2S)\text{-DPEN})](SbF_6)_2$ (**2**), which is a catalyst precursor for the hydrogenation of aryl ketones. Two epimers of **2**, R_{Ar},S,S and S_{Ar},S,S, are formed when starting from racemic **1**; this 1:1 mixture of diastereomers catalyzed the asymmetric hydrogenation of acetophenone. The enantiomerically pure diastereomers were obtained from resolved **1** and used separately to catalyze the reaction. Each diastereomer showed different selectivity, with S_{Ar},S,S-**2** being the more selective (61% ee for the hydrogenation of acetophenone). Our studies suggest that ruthenium hydride formation is accompanied by a decrease in hapticity of the η^6-arene and probable detachment of the ring from the metal. Nevertheless, the original conformational chirality of the biphenyl ligand appears to be at least partially retained during the catalysis.

Keywords: Catalysis; Memory effect; Fluxional; Ruthenium; Tether; Non-rigid

1. Introduction

The ruthenium catalyzed asymmetric hydrogenation of ketones developed by Noyori and coworkers [1–11] has emerged as a powerful method for the production of chiral non-racemic alcohols. These catalysts, which derive from complexes of the general form *trans*-$RuCl_2$(bisphosphine)(diamine) or *trans*-$RuCl_2$(phosphine)$_2$(diamine), are very active and selective for a variety of ketones [1–11]. The accepted mechanism involves a non-classical metal–ligand bifunctional catalysis, where the ancillary ligands play an active role in the reaction. Specifically, an *in situ* generated amido ligand is thought to aid in the activation of dihydrogen, and to then be involved in a proton transfer to the ketone [12–15]. There has been recent interest in systems in which the chirality of one ligand can be used to convey the chiral information to another conformationally flexible ligand [16–22]. A particularly effective case is that of $RuCl_2$(1*S*,2*S*-DPEN)(BIPHEP) where DPEN is configurationally stable diphenylethylenediamine and BIPHEP is dynamically chiral 2,2′-bis(diphenylphosphino)-1,1′-biphenyl [19].

During the course of our recent research with the planar chiral arene-tethered half-sandwich complex $Ru(\eta^6{:}\eta^1\text{-}NMe_2C_6H_4C_6H_4PCy_2)Cl_2$ (**1**) [23–25], we have found that a dicationic derivative, $[Ru(\eta^6{:}\eta^1\text{-}NMe_2C_6H_4C_6H_4PCy_2)((1S,2S)\text{-DPEN})](SbF_6)_2$ (**2**), is a catalyst precursor for the asymmetric hydrogenation of ketones under the conditions first reported by Noyori et al. [3], In **1** the configuration of the potentially dynamically chiral biphenyl ligand is locked in place by the coordination to the metal and the complex shows no propensity for racemization in solution. The dicationic complex, **2**, also retains its configuration in solution. As **2** is an 18-electron coordinately

* Corresponding author. Fax: +1 203 432 6144.
E-mail address: jack.faller@yale.edu (J.W. Faller).

0022-328X/$ - see front matter © 2006 Elsevier B.V. All rights reserved.
doi:10.1016/j.jorganchem.2006.11.010

saturated species, its activation during its use in catalytic hydrogenation must involve the generation of open coordination sites to facilitate the binding of the substrate and/or the formation of one or more hydrides. Our initial investigations have suggested that the loss of the η^6-arene ligand during the catalysis furnishes the necessary binding sites, though this occurs with a high degree of retention of the ligand chirality. This report details the preliminary characterization and catalysis with **2**, with an emphasis on the analysis of the chiral elements of the complex and their respective effects on the catalytic selectivity.

2. Results and discussion

The dicationic complex **2** was prepared by the abstraction of the two chloride ligands of **1** with $AgSbF_6$ in the presence of the chiral diamine (1*S*,2*S*)-DPEN. The resulting dicationic complex is a robust air stable yellow solid that can be readily handled on the bench top. When starting from racemic **1**, two diastereomers in a 1:1 ratio are formed owing to the fixed chirality of the diamine ligand (Scheme 1). The ^{1}H NMR spectrum shows that, for both of the two isomers ($R_{Ar}S,S$-**2** and $S_{Ar}S,S$-**2**), each of the four amino protons are diastereotopic at room temperature. The protons attached to the chelate ring are readily identified by the larger coupling constants (~12 Hz) from geminal coupling on the NH_2 groups and *trans* couplings between the axial NH's and CH's, whereas the η^6-arene ring protons generally have couplings of up to ~7 Hz. The broadening from the quadrupolar ^{14}N provides identification of the protons attached to nitrogen. Cross peaks in a COSY experiment provided the connectivity, as is indicated for the R_{Ar},R,R diastereomer, which is shown in Fig. 1. Identification of which amino protons are *syn* or *anti* to the dimethylamino substituents was not straightforward, although one might speculate that an upfield shift would be expected for the axial NH proton (H_{1a}) owing to the ring current from the η^6 ring.That the four amino protons are diastereotopic is indicative fairly strong bonds between the diamine and the ruthenium center. A dynamic process involving hemilability of the diamine would eliminate the diastereotopic nature of the amino protons in the

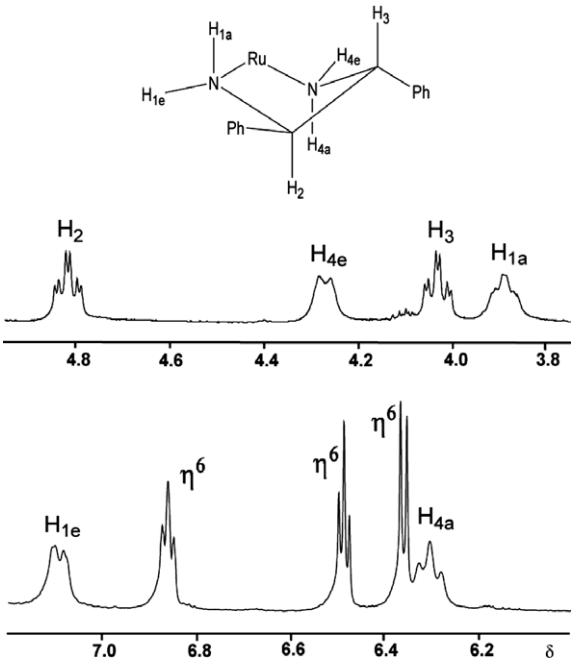

Fig. 1. Regions of the ^{1}H NMR Spectrum of R_{Ar},R,R-2.

NMR spectrum. Specifically, the dissociation of one of the amino ligands, which would result in a hemilabile 16-electron species, would at least make the two protons on the free amine equivalent owing to the fast N–C bond rotation and an umbrella-flip processes. That is, dissociation should allow for the facile interconversion of the two amino protons since the abovementioned dynamic processes would be expected to be fast relative to the NMR timescale upon the generation of a free amine and subsequent recoordination. The observance of four diastereotopic amino protons therefore precludes a hemilabile process that is fast on the NMR timescale.

Along these lines, the observance of the four diastereotopic amino protons reflects the differences in the two sides of the chelate. This is an effect of the planar chirality of the complex; more specifically, one of the amino groups is bound *syn* with respect to the NMe_2 moiety on the η^6-arene ring, while the other is *anti*. Here again, the rigidity of the complex is illustrated, as the aforementioned

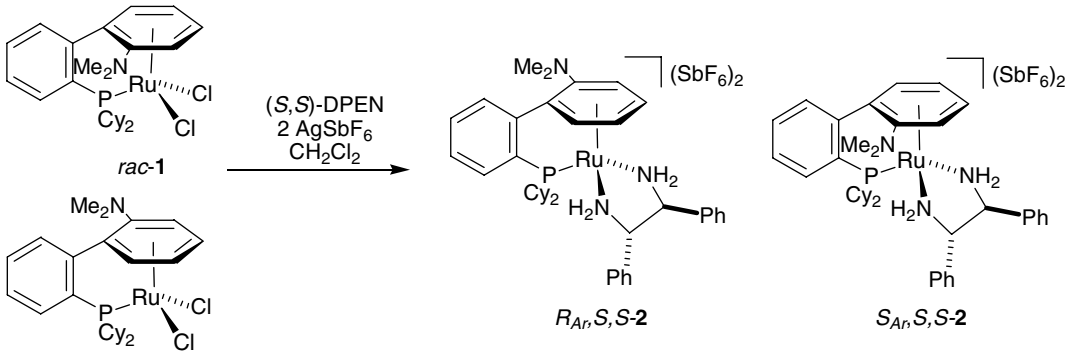

Scheme 1. Synthesis of **2**.

hemi-labile process could also potentially give rise to the interconversion of the two sides of the diamine. The non-labile nature of the DPEN ligand was further evidenced by elevated temperature NMR experiments in d^6-dmso, which showed the four amino protons remained diastereotopic even at a temperature of 125 °C, at which point no observable line broadening had occurred in any of the resonances. The inequivalency of these amino protons is a potentially important feature of **2**, since the amino ligands of ruthenium complexes are often cited as active participants in the catalytic hydrogenation reactions.

The two diastereomers, R_{Ar},*S*,*S*-**2** and S_{Ar},*S*,*S*-**2**, can be obtained individually by utilizing the BINAM-based resolution protocol that has been previously reported by our laboratory.[24] This process, which involves the similar diastereomeric complexes $[Ru(\eta^6{:}\eta^1\text{-}NMe_2C_6H_4C_6H_4P\text{-}Cy_2)((R)\text{-BINAM})](SbF_6)_2$ (**3**) provides a route to enantiopure **1**. While the diastereomers of **3** are resolvable by fractional crystallization, this is not feasible for the DPEN variants owing to the tendency for R_{Ar},*S*,*S*-**2** and S_{Ar},*S*,*S*-**2** to crystallize as a quasi-racemate. From the X-ray structure of the quasi-racemate (Fig. 2), it is clear that the phenyl groups on the backbone on DPEN are similarly disposed relative to the rest of the complex. Hence, the outside surface of the complex of either the (1*S*,2*S*) or (1*R*,2*R*)-DPEN would be very similar. Therefore, upon crystallization of the R_{Ar},*S*,*S*-**2** and S_{Ar},*S*,*S*-**2** diastereomeric mixture, the planar chiral arene-tethered ligands arrange themselves to be centrosymmetrically related in a pseudo-$P2_1/m$ array, which accounts for the observed formation of the quasi-racemate. The similarity of the phenyl orientations in diastereomers can be appreciated by comparing R_{Ar},*S*,*S*-**2**, with R_{Ar},*R*,*R*-**2** (Fig. 3.)

The complex **2**, although it is a coordinately saturated complex with no apparent fluxional behavior, is an efficient and asymmetric catalyst for the hydrogenation of acetophenone and 1′-acetonaphthone. The catalytic conditions are those first developed by Noyori and coworkers: under hydrogen pressure of 8 atm, in *i*-PrOH, and activated with an inorganic base [3]. The results are summarized in Table 1; the reaction does not proceed in the absence of either the H_2 pressure or the base. The 1:1 mixture of the two isomers, R_{Ar},*S*,*S*-**2** and S_{Ar},*S*,*S*-**2**, catalyzes the hydrogenation of acetophenone (**4a**) to furnish (+)-(*R*)-*sec*-phenethyl alcohol (**5a**) in 51% enantiomeric excess (ee). The more bulky aromatic group in acetonaphthone (**4b**) did not adversely affect the conversion, although the ee was lower (34%) when again the reaction was catalyzed by the diastereomeric mixture of **2**.

Interestingly, the BINAM variant, **3**, results in only 3% conversion to product under the identical conditions. This may be related to the increased lability of the BINAM ligand with respect to DPEN, which is reflected in the comparative instability of **3**. For example, while **2** is stable in untreated solutions for extended periods, **3** undergoes facile decomposition in a variety of solvents, and in general is best handled in dry CH_2Cl_2 and under a nitrogen atmosphere.

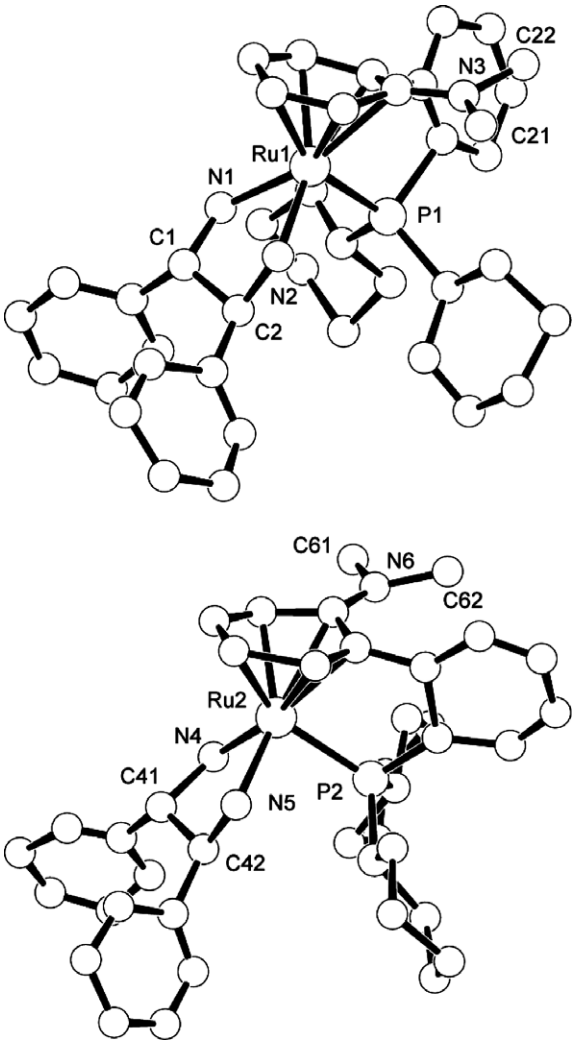

Fig. 2. ORTEP diagrams of the cations in R_{Ar},*S*,*S*-2 (top) and S_{Ar},*S*,*S*-2 (bottom) from the quasi-racemate.

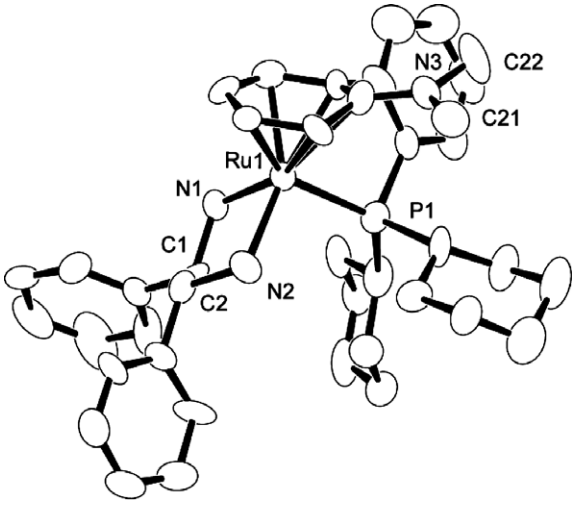

Fig. 3. An ORTEP diagram of the cation of R_{Ar},*R*,*R*-2 from enantiomerically pure material.

Table 1
Catalytic hydrogenations of ketones

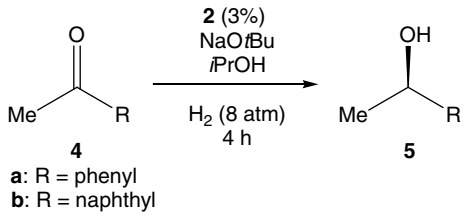

Entry	Precatalyst	Ketone	Conversion (%)	ee
1	1:1 Mix (R_{Ar},*S*,*S*)-**2**/(S_{Ar},*S*,*S*)-**2**	**4a**	>98	51
2	1:1 Mix (R_{Ar},a*R*)-**3**/(S_{Ar},a*R*)-**3**	**4a**	3	N/A
3	(R_{Ar},*S*,*S*)-**2**	**4a**	>98	40
4	(S_{Ar},*S*,*S*)-**2**	**4a**	>98	61
5	1:1 Mix (R_{Ar},*S*,*S*)-**2**/(S_{Ar},*S*,*S*)-**2**	**4b**	>98	34
6	(R_{Ar},*S*,*S*)-**2**	**4b**	>98	27
7	(S_{Ar},*S*,*S*)-**2**	**4b**	>98	40

All hydrogenations were carried out at a catalyst concentration of 0.02 M, with a 20:1 base to catalyst ratio.

The relative lability of BINAM is further illustrated by the reaction shown in Scheme 2, where the addition of an equivalent of DPEN to a CD_2Cl_2 solution of **3** resulted in the facile and quantitative conversion to **2** within 30 min. The partial precipitation of **2** may have helped to drive the reaction to completion; nonetheless, the relative ease with which the BINAM ligand is displaced reflects its lability in solution. Given this, it is unlikely that the BINAM ligand in **3** would remain bound to ruthenium under the catalytic conditions. This could also suggest that the DPEN ligand in **2** may actively participate in the hydrogenation reaction.

When the diastereomers of **2** are used individually in the hydrogenation of **4a**, in both cases (+)-(*R*)-**5a** is produced, although the ee was slightly different in each case. Specifically, the ee was improved for S_{Ar},*S*,*S*-**2** (61%) and worsened for R_{Ar},*S*,*S*-**2** (40%). This trend holds for both of the ketone substrates (**4a**–**4b**), and in both cases the selectivity of the reaction catalyzed by the mixture of isomers was approximately the average of the selectivity given by the two isomers individually. This implies that the reaction rates are nearly the same for the two diastereomeric precatalysts. While it is clear from this that the most important element in the transfer of chirality is the DPEN chelate, it is noteworthy that the two isomers of **2** impart different enantioselectivity to the catalytic reaction, and that a higher selectivity was noted in the case of S_{Ar},*S*,*S*-**2**. The implication is that the planar chiral arene-tethered ligand is also affecting the selectivity.

This result provides a clue to the nature of the true catalyst; since both chiral elements are involved in the chiral transfer, it suggests that both remain bound during the reaction. Since the precursor **2** is coordinately saturated, binding sites must be generated during the course of the catalysis by the dissociation (or partial dissociation) of one or more of the ligands. The ^{1}H NMR of the crude mixture after a hydrogenation catalyzed by the 1:1 mix of the diastereomers of **2** showed no sign of any η^6 resonances, which generally appear between 4 and 7 δ. In addition, small amounts of two hydride resonances were observed in an approximate ratio of 2:1, both of which were doublets of ~37 Hz due to phosphorus coupling. Unfortunately, the rapid decomposition of the hydride species prevented more complete characterization. The lack of η^6 resonances in the post-catalytic mixture suggests that the formation of the hydride(s) is accommodated by the dissociation of the arene during the catalysis. There is a precedent for the dissociation of η^6-arene ligands under similar conditions; early work done by Noyori and co-workers showed that complexes of the type [Ru(η^6-arene)(BINAP)X]$^+$ were hydrogenation catalyst precursors in which coordinately unsaturated species were formed by liberation of the η^6-arene [26]. In this case, due to the tethering of the arene, its dissociation could give rise to a P–N binding mode. The hydride resonances in the crude catalytic mixture are potentially due to an isomeric mixture caused by a flexible P–N bonding mode (Fig. 4). Since R_{Ar},*S*,*S*-**2** and S_{Ar},*S*,*S*-**2** catalyzed the reaction with different selectivity, though, it can be said for certain that the chirality of the ligand is retained (at least to a large extent) even if the arene is completely dissociated.

That the η^6:η^1 binding mode effectively halts the atropisomeric interconversion of the biphenyl ligand is evidenced by the configurational stability of **1**, for which no observable racemization occurs. This contrasts with the flexible nature of the free ligand, for which a free energy of activation of 18.8 kcal/mol has been reported by our laboratory [27]. This barrier is sufficiently low as to prevent the resolution of the free ligand, since racemization occurs within a

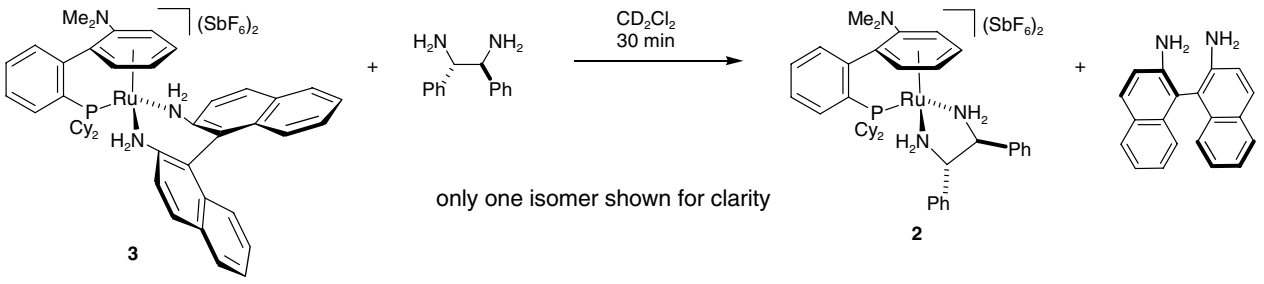

Scheme 2. Conversion of **3** into **2**.

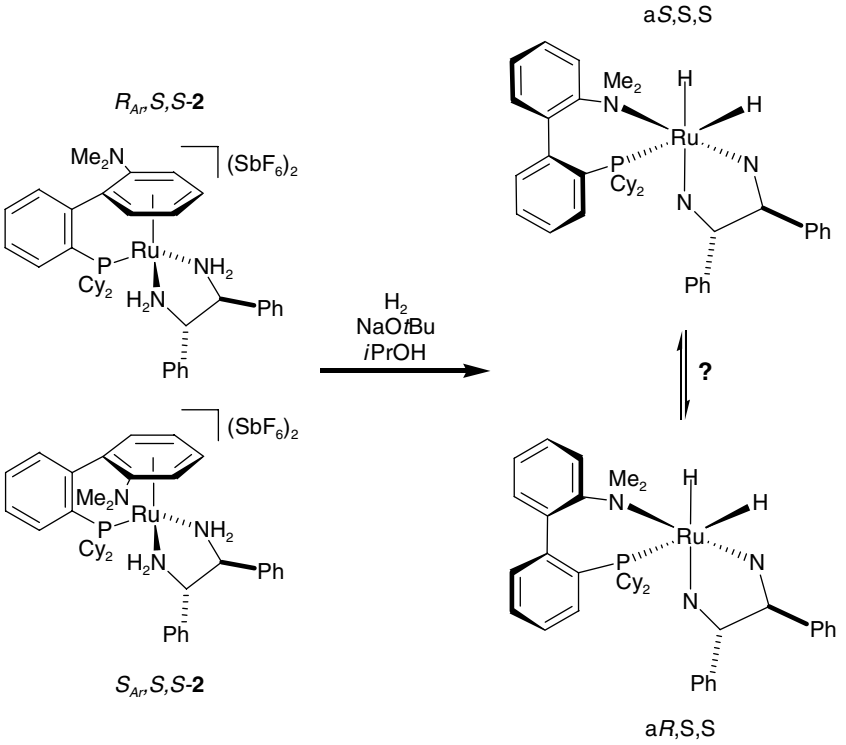

Fig. 4. Possible atropisomeric mixture of catalyst. One possible geometry for activation of the complex by ring-slippage upon addition of H_2. Note that the initial retention of the chirality in the P–N ligand results in diastereomeric complexes for a given metal geometry.

few seconds. The P–N binding mode serves to increase the barrier; for example, we have previously described the preparation of (η^3-allyl)Pd(η^1:η^1- $NMe_2C_6H_4C_6H_4PPh_2$), which has a free energy of activation of ~22 kcal/mol [27]. The similar complex (η^3-allyl)Pd(η^1:η^2- $NMe_2C_6H_4$-$C_6H_4PCy_2$) exhibited a somewhat unusual binding mode involving an η^2-aryl interaction with an aromatic ring, though the free energy of activation for the dynamically chiral ligand was thought to be the same (~22 kcal/mol) as with the other complex with the P–N mode [27]. Therefore, this type of η^2-aryl binding, which has also been observed in some ruthenium compounds [28–36], cannot be ruled out in the present case. While an appreciable increase in the interconversion barrier of the ligand would be expected from either binding mode, the racemization half-life for a barrier of 22 kcal/mol is still on the order of ~12 min at room temperature, which is below the limit of what is typically considered atropisomerism [37].

From this, if the active catalyst for the hydrogenation reaction involves a P–N bonding mode, then it is feasible that the epimerization of the metal complex could be occurring at a comparable rate to the catalysis. That R_{Ar},*S*,*S*-**2** and S_{Ar},*S*,*S*-**2** give different selectivity in the reaction, however, shows that the stereochemistry of the catalysts is under kinetic control. That is, if a complete equilibration occurred much faster than the rate of the hydrogenation reaction, then the two isomers would produce the same selectivity. Although the catalyses were generally allowed to react for 4 h, it was later noted that the hydrogenation of **4a** was complete within 30 min. When the hydrogenation of acetophenone, catalyzed by S_{Ar},*S*,*S*-**2**, was halted after 10 min, the reaction was seen to have proceeded to 39% conversion. At this point, **5a** was produced in the same ee as at the end of the reaction (61%), so the selectivity of the catalyst remains constant during the course of the reaction under these conditions. After 15 min, the reaction had proceeded to 91% conversion, and so it appears that after a short induction period the reaction occurs over a very brief interval of time.

Therefore, this is a different effect from what has been successfully implemented by Mikami and co-workers [19,38], which involves an equilibration of a dynamically chiral ligand prior to catalysis. In this case it seems that, for the standard conditions, the hydrogenation reaction occurs very quickly in comparison to the epimerization of the catalyst. When additional ketone (3 × the usual amount, a 100-fold excess with respect to the catalyst) was added to the reaction catalyzed once again with S_{Ar},*S*,*S*-**2**, while keeping the catalyst and base concentrations the same as with the prior runs, the ee of **5a** decreased to 55% at complete conversion. If the turnover-limiting step is the hydride formation, as is often the case, then the addition of excess ketone while holding the other reactant concentrations constant should serve to extend the reaction time. Indeed, kinetic studies on Noyori's system have indicated that the reaction rate is generally independent of the initial substrate concentration [15]. On this basis, we postulate that the decrease in enantioselectivity

is due to a longer reaction time, which allows for the epimerization of the catalyst to become a factor.

3. Conclusions

In summary [Ru(η^6:η^1- $NMe_2C_6H_4C_6H_4PCy_2$)((1*S*,2*S*)-DPEN)][SbF_6)$_2$ (**2**) is an efficient and asymmetric catalyst for the hydrogenation of acetophenone and 1′-acetonaphthone. This is in contrast to [Ru(η^6:η^1- $NMe_2C_6H_4C_6H_4PCy_2$)((*R*)- BINAM)][SbF_6)$_2$ (**3**), which shows very little activity under the same conditions. The reason for this marked difference in behavior could be related to the increased lability of BINAM in comparison to DPEN. The DPEN chelate is in fact quite rigidly bound, as evidenced by high temperature NMR experiments, which showed that no exchange of the four diastereotopic amino protons occurred in d^6-dmso up to 125 °C.

The results of the catalyses showed that in fact the dominant chiral element of the catalyst is the (*S*,*S*)-DPEN chelate. This was established by a comparison of the enantioselectivity of hydrogenation reactions catalyzed by R_{Ar},*S*,*S*-**2**, S_{Ar},*S*,*S*-**2**, and the 1:1 mix of these two diastereomers, which all furnished the (*R*)-alcohols with different ee's. The fact that (*R*)-alcohols were obtained in excess in each case shows that the fixed chirality of (*S*,*S*)-DPEN is overriding the mixed chirality of the arene-tethered ligand. That the diamine is the most important feature in stereocontrol, and that the catalyst is activated with an alkoxide base, suggests a metal–ligand bifunctional mechanism, where the *in situ* generated amido ligands are active participants in the reaction.

That each isomer separately gave different selectivity demonstrates that the chirality of the arene-tethered ligand *does influence* the chiral transfer, and so it can be said that the memory of this chirality is retained during the reaction. The NMR of the post-catalytic mixture showed two hydride resonances in unequal proportions, and an apparent lack of resonances that would correspond to η^6-protons. The rapid decomposition of this crude mixture has prevented our further characterization of these species; however, we propose the dissociation of the η^6-arene, possibly yielding a P–N binding mode, to account for the generation of the sites necessary to accommodate the reaction. Thus, the true catalyst may be of the form Ru(diamine)-(phosphine-amine), which is a novel catalyst type, and represents an extension to Noyori's catalyst class. Future work will focus on further mechanistic examinations, as well as on the modification of this catalyst system to increase the selectivity and extend the scope.

4. Experimental

4.1. General

The manipulations were carried out under a nitrogen atmosphere using standard Schlenk techniques. Isopropyl alcohol was dried over CaH_2 lumps (4 mesh) and purged with nitrogen prior to use. CH_2Cl_2 was distilled over CaH_2 under a nitrogen atmosphere. (1*S*,2*S*)-DPEN, (1*R*,2*R*)-DPEN, (*R*)-BINAM, $AgSbF_6$ (Strem), acetophenone, aectonaphthone, NaO*t*-Bu, Et_2O, and Eu(hfc)$_3$ (Aldrich), were all used as received. NMR spectra were recorded on a Bruker 400 MHz (operating at 162 MHz for ^{31}P), or a Bruker 500 MHz (operating at 202 MHz for ^{31}P). Chemical shifts are reported in ppm relative to solvent peaks (^{1}H), or an H_3PO_4 external standard. The elemental analysis of **2** was performed by Atlantic Microlabs.

4.2. Nomenclature

Chirality descriptors for planar chirality are usually indicated by *pS* and *pR*,however the convention for η^6-arene organometallics is to specify the chirality based on the highest priority carbon attached to the metal and *p* is not used. In the case at hand, it is difficult to distinguish the chirality descriptor of the arene portion from that of the diamine ligand and there do not appear to be precedents for describing this. It would not be appropriate to use S_{Ru} since that descriptor is based on a stereogenic ruthenium atom, not the carbon of the arene. We have placed the arene descriptor first, followed by that of the ligand. In order to distinguish the arene metal chirality from that of the ligand we have used a descriptor with an "Ar" subscript (*e.g.* R_{Ar},*R*,*R*).

4.3. Synthesis of [Ru(η^6:η^1-$NMe_2C_6H_4C_6H_4PCy_2$)((1*S*,2*S*)-DPEN)][SbF_6)$_2$ (**2**)

A flame-dried flask was charged with **1** (60 mg, 0.11 mmol) and $AgSbF_6$ (74 mg, 0.22 mmol) under a stream of nitrogen. CH_2Cl_2 (4 mL) was then added, followed by (1*S*,2*S*)-DPEN (23 mg, 0.11 mmol). The resulting mixture was stirred for 1/2 h, over which time a bright yellow color develops. The mixture was then filtered through Celite, eluting with acetone, and dried under vacuum. Crystals were obtained by slow diffusion of Et_2O into a CH_2Cl_2 solution. Anal. Calc. for $C_{40}H_{52}F_{12}N_3PRuSb_2$: C, 40.77; H, 4.45; N, 3.57. Found: C, 40.59; H, 4.46; N, 3.45%. Crystals suitable for X-ray determination were obtained from diffusion of Et_2O into an acetone solution.

4.4. (S_{Ar}*S*,*S*)-**2**

^{1}H NMR (500 MHz, $(CD_3)_2CO$): 8.19 (1H, m), 8.05 (1H, m), 7.82 (2H, m), 7.48–7.40 (4H, m), 7.36–7.24 (6H, m), 7.09 (1H, br dd, $J = 12$ Hz, 4 Hz, NH_2), 6.86 (1H, m, C$H_{\eta 6\text{-arene}}$), 6.49 (1H, t, $J = 5.6$ Hz, C$H_{\eta 6\text{-arene}}$), 6.36 (1H, d, $J = 6.8$ Hz, C$H_{\eta 6\text{-arene}}$), 6.31 (br t, $J = 12$ Hz, NH_2), 5.59 (1H, d, $J = 5.6$ Hz, C$H_{\eta 6\text{-arene}}$), 4.82 (1H, td, $J = 12.0$, 4.4 Hz, C(Ph)H_{DPEN}), 4.27 (1H, br t, $J = 12$ Hz, NH_2), 4.03 (1H, td, $J = 12.0$, 4.0 Hz, C(Ph)H_{DPEN}), 3.89 (1H, br t, $J = 12$ Hz, NH_2), 2.97 (1H, m, C$H_{cyclohexyl}$), 2.79 (1H, m, C$H_{cyclohexyl}$), 2.75 (6H, s, N(CH_3)$_2$), 2.26

(1H, m, C$H_{2cyclohexyl}$), 2.17 (2H, m, C$H_{2cyclohexyl}$), 1.95 (1H, m, C$H_{2cyclohexyl}$), 1.91–1.13 (12H, m, C$H_{2cyclohexyl}$), 0.98–0.82 (4H, m, C$H_{2cyclohexyl}$). ^{31}P NMR (202 MHz, $(CD_3)_2CO$): 57.3.

4.5. (R_{Ar},S,S-2)

^{1}H NMR (400 MHz, $(CD_3)_2CO$): 8.18 (1H, m), 8.08 (1H, m), 7.82 (2H, m), 7.48–7.43 (4H, m), 7.35–7.25 (6H, m), (CH_{arom}); 7.13 (1H, br d, $J = 12$ Hz, NH_2), 6.86 (1H, tt, $J = 6.4$ Hz, 1.6 Hz, C$H_{\eta 6\text{-arene}}$), 6.82 (1H, m, C$H_{\eta 6\text{-arene}}$), 6.54 (br t, $J = 12$ Hz, NH_2), 5.92 (1H, d, $J = 6.4$ Hz, C$H_{\eta 6\text{-arene}}$), 5.69 (1H, br d, $J = 12$ Hz, NH_2), 5.68 (1H, dd, $J = 5.3$ Hz, 1.3 Hz, C$H_{\eta 6\text{-arene}}$), 4.80 (1H, td, $J = 12.0$, 4.0 Hz, C(Ph)H_{DPEN}), 4.13 (1H, td, $J = 11.9$, 4.2 Hz, C(Ph)H_{DPEN}), 3.14 (1H, m, C$H_{cyclohexyl}$), 2.78 (1H, br t, $J = 12$ Hz, NH_2), 2.68 (6H, s, NMe_2), 2.55–2.48 (2H, m, C$H_{cyclohexyl}$ and C$H_{2cyclohexyl}$), 2.14 (1H, m, C$H_{2cyclohexyl}$), 2.00–1.20 (13H, m, C$H_{2cyclohexyl}$), 1.10–1.01 (2H, m, C$H_{2cyclohexyl}$), 0.92–0.83 (2H, m, C$H_{2cyclohexyl}$), 0.66 (1H, m, C$H_{2cyclohexyl}$). ^{31}P NMR (162 MHz, $(CD_3)_2CO$): 57.7.

4.6. Synthesis of [(R)-Ru(η^6:η^1-N$Me_2C_6H_4$-$C_6H_4PCy_2$)((1R,2R)-DPEN)]$(SbF_6)_2$ (R_{Ar},R,R-2)

This complex was synthesized using enantiomerically pure (*R*)-**1** as above. Crystals suitable for X-ray determination were obtained by slow diffusion of Et_2O into an acetone solution.

4.7. Catalytic ketone hydrogenation

A flame-dried flask was charged with **2** (8.8 mg, 0.0075 mmol), and NaO*t*-Bu (14 mg, 0.15 mmol), and placed under a nitrogen atmosphere. *i*-PrOH (3.75 mL) was then added, followed by the appropriate ketone (0.25 mmol), and the solution was stirred for 5 min before it pressurized with H_2 (8 atm) for 4 h. After this time, the mixture was removed from the bomb, diluted with Et_2O (20 mL), and passed through a short column of silica eluting with more Et_2O. The resulting solution was dried under vacuum, the conversion was determined by integration of the resulting ^{1}H NMR spectrum. The ee was determined with the addition of the chiral shift agent (+)-Eu(hfc)$_3$ in C_6D_6; it was observed that for both of the product alcohols the α-proton split after 6.0 ppm, and the more downfield resonance correlated with the (*R*)-alcohol.

4.8. Conversion of 3 into 2

A flame-dried flask was charged with **3** (35 mg, 0.028 mmol, 1:1 mixture of diastereomers) and (1*S*,2*S*)-DPEN (6.0 mg, 0.028 mmol), and was placed under a nitrogen atmosphere. CD_2Cl_2 (0.5 mL, degassed) was then added, resulting in an orange solution that gradually turned yellow and developed a precipitate over 30 min. At this time, the solvent was removed under vacuum, and the residue was extracted with Et_2O to remove the BINAM. The resulting yellow residue was dried under vacuum, furnishing the 1:1 diastereomeric mix of **2** (32 mg, 97%).

4.9. Crystal structure determination and refinement

Data were collected on a Nonius KappaCCD (Mo Kα radiation) diffractometer and scaled using HKL2000 [39,40]. The data were not specifically corrected for absorption other than the inherent corrections provided by Scalepack [40]. The structures were solved by direct methods (SIR92) and refined on *F* for all reflections.[41,42] Non-hydrogen atoms were refined with anisotropic displacement parameters. Hydrogen atoms were included at calculated positions. Non-hydrogen atoms were refined with anisotropic displacement parameters for R_{Ar},*R*,*R*-**2**. Hydrogen atoms were included at calculated positions. Both structures contained disordered ether molecules and the data were adjusted to remove their contribution to the scattering using SQUEEZE in the program PLATON [43]. Owing to the pseudo symmetry there was difficulty refining the individual isomers owing to correlations and therefore the carbon atoms in quasiracemate-**2** were refined isotropically. The structures of the two diastereomeric cations found in the quasiracemate have been shown in Fig. 2. The structure of one of two independent cations of the pure enantiomer of R_{Ar},*R*,*R*-**2** is shown in Fig. 3. The absolute configurations of the diastereomers of **2** are based on the known *S*,*S*, configuration of DPEN. Owing to pseudosymmetry providing a near centrosymmetric placement of heavy atoms.

The determination of configuration by anomalous dispersion is difficult (correct $R = 0.0549$, $R_w = 0.0572$; inverted $R = 0.0552$, $R_w = 0.0575$). For R_{Ar},*R*,*R*-**2**, the known configuration of *R*,*R*-DPEN establishes the absolute configuration; however, the configuration is also established by *R* factors with inversion of coordinates (correct $R = 0.0459$, $R_w = 0.0478$; inverted $R = 0.0491$, $R_w = 0.0529$). Relevant crystal and data parameters are presented in Table 2. The metrical parameters for the quasiracemate are not reliable owing to the correlations; however those for the two cations in R_{Ar},*R*,*R*-**2** are given in Table 3. Owing to disorder and the problems of pseudosymmetry the thermal parameters are larger than would be ideal and the metrical parameters less accurate; nevertheless the essential features of the structures are evident in the quasiracemate.

Appendix A. Supplementary material

CCDC 618862 and 618863 contain the supplementary crystallographic data for R_{Ar},*R*,*R*-**2** and R_{Ar}/S_{Ar},*S*,*S*-**2**. These data can be obtained free of charge via http://www.ccdc.cam.ac.uk/conts/retrieving.html, or from the Cambridge Crystallographic Data Centre, 12 Union Road,

Table 2
Crystallographic data for **2**

	$R_{Ar}/S_{Ar},S,S$-**2**	R_{Ar},R,R-**2**
Color, shape	Orange, block	Orange, needle
Empirical formula	$C_{47}H_{68}F_{12}N_3O_2PRuSb_2$	$C_{49}H_{74}F_{12}N_3O_2PRuSb_2$
Formula weight	1310.60	1411.57
Radiation/Å	Mo Kα (monochr.) 0.71073	Mo Kα (monochr.) 0.71073
T/K	173	173
Crystal system	Monoclinic	Monoclinic
Space group	$P2_1$ (No. 4)	$P2_1$ (No. 4)
Unit cell dimensions		
a/Å	13.6267(3)	13.7472(3)
b/Å	16.9768(4)	16.5373(4)
c/Å	23.2927(6)	23.7835(5)
β/°	95.675(2)	96.478(2)
V/Å^3	5362.1(2)	5372.5(2)
Z	4	4
D_{calc}/g cm^{-3}	1.623	1.745
μ/cm^{-1} (Mo Kα)	13.87	14.87
Crystal size/mm	$0.14 \times 0.17 \times 0.19$	$0.10 \times 0.10 \times 0.12$
Total reflections, unique reflections	21,198, 12,604	22,053, 12,703
R_{int}	0.059	0.039
Number of observations (I) > 3σ(I)	9432	13,601
Parameters, constraints	662, 0	1116, 0
R[a], R_w[b], GOF	0.055, 0.057, 1.89	0.046, 0.048, 1.79
Residual density/ e Å^{-3}	−0.80 < 0.73	−0.86 < 0.75

[a] $R_1 = \sum ||F_o| - |F_c|| / \sum |F_o|$, for all $I > 3\sigma(I)$.
[b] $R_w = [\sum[w(|F_o| - |F_c|)^2] / \sum[w(F_o)^2]]^{1/2}$.

Table 3
Selected bond length and angles for the two independent ions in R_{Ar},R,R-**2**

	Ion **1**	Ion **2**
Bond length (Å)		
Ru1–P1, Ru2–P2	2.353(2)	2.355(2)
Ru1–N1, Ru2–N4	2.129(6)	2.153(6)
Ru1–N2, Ru2–N5	2.142(7)	2.172(8)
Bond angles (°)		
N1–Ru–N2, N4–Ru–N5	78.2(2)	78.2(2)
N1–Ru–P1, N5–Ru–P2	94.2(2)	89.6(2)
N2–Ru–P1, N4–Ru–P2	99.0(2)	100.9(2)

Cambridge CB2 1EZ, UK; fax: (+44) 1223-336-033; or e-mail: deposit@ccdc.cam.ac.uk. Supplementary data associated with this article can be found, in the online version, at doi:10.1016/j.jorganchem.2006.11.010.

References

[1] H. Doucet, T. Ohkuma, K. Murata, T. Yokozawa, M. Kozawa, E. Katayama, A.F. England, T. Ikariya, R. Noyori, Angew. Chem., Int. Ed. 37 (1998) 1703.
[2] T. Ohkuma, D. Ishii, H. Takeno, R. Noyori, J. Am. Chem. Soc. 122 (2000) 6510.
[3] T. Ohkuma, H. Ooka, S. Hashiguchi, T. Ikariya, R. Noyori, J. Am. Chem. Soc. 117 (1995) 2675.
[4] T. Ohkuma, H. Ooka, M. Yamakawa, T. Ikariya, R. Noyori, J. Org. Chem. 61 (1996) 4872.
[5] R. Noyori, T. Ohkuma, Pure Appl. Chem. 71 (1999) 1493.
[6] T. Ohkuma, M. Koizumi, H. Doucet, T. Pham, M. Kozawa, K. Murata, E. Katayama, T. Yokozawa, T. Ikariya, R. Noyori, J. Am. Chem. Soc. 120 (1998) 13529.
[7] T. Ohkuma, H. Doucet, T. Pham, K. Mikami, T. Korenaga, M. Terada, R. Noyori, J. Am. Chem. Soc. 120 (1998) 1086.
[8] T. Ohkuma, M. Koizumi, M. Yoshida, R. Noyori, Org. Lett. 2 (2000) 1749.
[9] T. Ohkuma, M. Koizumi, H. Ikehira, T. Yokozawa, R. Noyori, Org. Lett. 2 (2000) 659.
[10] T. Ohkuma, T. Hattori, H. Ooka, T. Inoue, R. Noyori, Org. Lett. 6 (2004) 2681.
[11] T. Ohkuma, C.A. Sandoval, R. Srinivasan, Q. Lin, Y. Wei, K. Muniz, R. Noyori, J. Am. Chem. Soc. 127 (2005) 8288.
[12] K. Abdur-Rashid, S.E. Clapham, A. Hadzovic, J.N. Harvey, A.J. Lough, R.H. Morris, J. Am. Chem. Soc. 124 (2002) 15104.
[13] K. Abdur-Rashid, M. Faatz, A.J. Lough, R.H. Morris, J. Am. Chem. Soc. 123 (2001) 7473.
[14] S.E. Clapham, A. Hadzovic, R.H. Morris, Coord. Chem. Rev. 248 (2004) 2201.
[15] C.A. Sandoval, T. Ohkuma, K. Muniz, R. Noyori, J. Am. Chem. Soc. 125 (2003) 13490.
[16] P.J. Walsh, A.E. Lurain, J. Balsells, Chem. Rev. 103 (2003) 3297.
[17] M.T. Reetz, X.G. Li, Angew. Chem., Int. Ed. 44 (2005) 2959.
[18] K. Mikami, K. Alkawa, Org. Lett. 4 (2002) 99.
[19] K. Mikami, T. Korenaga, M. Terada, T. Ohkuma, T. Pham, R. Noyori, Angew. Chem., Int. Ed. 38 (1999) 495.
[20] O. Corminboeuf, L. Quaranta, P. Renaud, M. Liu, C.P. Jasperse, M.P. Sibi, Chem.-Eur. J. 9 (2003) 29.
[21] J. Balsells, P.J. Walsh, J. Am. Chem. Soc. 122 (2000) 1802.
[22] J.W. Faller, J.C. Wilt, J. Organometal. Chem. 691 (2006) 2207.
[23] J.W. Faller, D.G. D'Alliessi, Organometallics 22 (2003) 2749.
[24] J.W. Faller, P.P. Fontaine, Organometallics 24 (2005) 4132.
[25] J.W. Faller, P.P. Fontaine, J. Organometal. Chem. 691 (2006) 1912.
[26] K. Mashima, K.H. Kusano, T. Ohta, R. Noyori, H. Takaya, Chem. Commun. (1989) 1208.
[27] J.W. Faller, N. Sarantopoulos, Organometallics 23 (2004) 2008.
[28] H. Aneetha, M. Jimenez-Tenorio, M.C. Puerta, P. Valerga, K. Mereiter, Organometallics 21 (2002) 628.
[29] N. Feiken, P.S. Pregosin, G. Trabesinger, A. Albinati, G.L. Evoli, Organometallics 16 (1997) 5756.
[30] N. Feiken, P.S. Pregosin, G. Trabesinger, Organometallics 16 (1997) 3735.
[31] N. Feiken, P.S. Pregosin, G. Trabesinger, M. Scalone, Organometallics 16 (1997) 537.
[32] T.J. Geldbach, P.S. Pregosin, A. Albinati, F. Rominger, Organometallics 20 (2001) 1932.
[33] T.J. Geldbach, P.S. Pregosin, Eur. J. Inorg. Chem. (2002) 1907.
[34] T.J. Geldbach, D. Drago, P.S. Pregosin, J. Organometal. Chem. 643 (2002) 214.
[35] T.J. Geldbach, P.S. Pregosin, A. Albinati, Organometallics 22 (2003) 1443.
[36] T.J. Geldbach, F. Breher, V. Gramlich, P.G.A. Kumar, P.S. Pregosin, Inorg. Chem. 43 (2004) 1920.
[37] M. Oki, Top. Stereochem. 14 (1983) 1.
[38] K. Mikami, K. Aikawa, Y. Yusa, J.J. Jodry, M. Yamanaka, Synlett (2002) 1561.
[39] W. Minor, Z. Otwinowski (Eds.), HKL2000 (Denzo-SMN) software package, Processing of X-ray Diffraction Data Collected in Oscillation Mode, Methods in Enzymology, Macromolecular Crystallography, Academic Press, New York, 1997.
[40] Z. Otwinowski, W. Minor, in: E. Arnold, (Ed.), International Tables for Crystallography; Vol. F, 2001.
[41] A. Altomare, G. Cascarano, C. Giacovazzo, A. Guagliardi, J. Appl. Crystallogr. 26 (1993) 343.
[42] TEXSAN, TEXSAN for Windows Version 1.06: Crystal Structure Analysis Package, Molecular Structure Corporation (1997-9), 1999.
[43] A.L. Spek, Acta Crystallogr. Sect. A 46 (1990) C34.